IEEE Access
SPECIAL SECTION ON EMERGING TRENDS, ISSUES AND CHALLENGES FOR ARRAY SIGNAL PROCESSING AND ITS APPLICATIONS IN SMART CITY

Received March 12, 2019, accepted April 1, 2019, date of publication April 9, 2019, date of current version April 19, 2019.

Digital Object Identifier 10.1109/ACCESS.2019.2909760

Tensor-Based Angle and Array Gain-Phase Error Estimation Scheme in Bistatic MIMO Radar

YUEHAO GUO[1], XIANPENG WANG[1], (Member, IEEE), LIANGTIAN WAN[2], (Member, IEEE), MENGXING HUANG[1], CHONG SHEN[1], KUN ZHANG [1], AND YONGQIN YANG[1]

[1]State Key Laboratory of Marine Resource Utilization in South China Sea, College of Information Science and Technology, Hainan University, Haikou 570228, China
[2]Key Laboratory for Ubiquitous Network and Service Software of Liaoning Province, School of Software, Dalian University of Technology, Dalian 116620, China

Corresponding authors: Xianpeng Wang (wxpeng1986@126.com) and Liangtian Wan (wanliangtian@dlut.edu.cn)

This work was supported in part by the Natural Science Foundation of Hainan Province under Grant 617059, in part by the National Natural Science Foundation of China under Grant 61701144, Grant 61801076, and Grant 61861015, in part by the Program of Hainan Association for Science and Technology Plans to Youth R&D Innovation under Grant QCXM201706, in part by the scientic research projects of University in Hainan Province under Grant Hnky2018ZD-4, in part by the Young Elite Scientists Sponsorship Program by CAST under Grant 2018QNRC001, and in part by the Scientic Research Setup Fund of Hainan University under Grant KYQD (ZR)1731.

ABSTRACT This paper investigates the issue of angle and array gain-phase error estimation in multiple-input-multiple-output (MIMO) radar, and a tensor-based angle and gain-phase error estimation scheme is proposed. In our approach, the parallel factor (PARAFAC) decomposition is performed to estimate the transmit and receive direction matrices. Then the estimation of gain error can be obtained according to the relationship between the columns of direction matrices. After that, the linear feature of the phase in the additional well-calibrated array element is utilized to estimate the angles. Finally, by fully using the phase characteristics of all arrays, the phase error can be obtained. Our approach can remove the influence of error accumulation, and thus it has a superior angle and gain-phase error estimation performance, particularly under the condition of low signal-to-noise ratio (SNR). The numerical examples validate the superiority and effectiveness of the proposed scheme.

INDEX TERMS Bistatic MIMO radar, angle estimation, gain-phase error, parallel factor decomposition.

I. INTRODUCTION

Angle estimation is a popular research topic in multiple-input multiple-output (MIMO) radar system, and it has attracted a lot of attention [1], [2]. Due to the fact that the virtual arrays can be generated in MIMO radar, the array aperture is enlarged and the number of array elements is increased. Thus the parameter estimation performance of MIMO radar system is more superior than that of conventional phased array radar [3]. On the basis of the configuration of transmit and receive arrays, MIMO radar is roughly grouped into two kinds. The transmit and received arrays equipped with close spacing between the antennas is called collocated MIMO radar [4]–[6]. On the contrary, The transmit and received arrays consisting of wide spacing between antennas is named as statistical MIMO radar [7]–[8]. The bistatic MIMO radar, which is investigated in this paper, is a collocated MIMO radar.

During the past few years, a large number of scholars have devoted their efforts to the issue of joint direction-of-departure (DOD) and direction-of-arrival (DOA) estimation in bistatic MIMO radar [9]–[12]. The two-dimensional Capon method has been investigated in [13], [14], and the DOD and DOA are paired automatically. However, the calculation complexity of this algorithm is relatively high due to the two-dimensional spatial spectrum searching. Similarly, the multiple signal classification (MUSIC) algorithm proposed in [15]–[17] also requires the two-dimensional spatial spectrum searching operation. To realize the purpose of reducing the computational complexity, a lot of methods without spatial spectrum searching is proposed in [18]–[26]. In [18]–[22], the estimation method of signal parameter via rotational invariance techniques (ESPRIT) is employed to achieve the angle estimation. These algorithms make use of the rotational invariance of the subspace to achieve the joint DOD and DOA estimation without the additional pairing procedure. In [23]–[26], the parallel factor (PARAFAC) method is used to achieve the angle estimation in MIMO radar systems. In these methods, the direction matrices are

The associate editor coordinating the review of this manuscript and approving it for publication was Wei Liu.

obtained firstly, and then the angle can be estimated through using the feature of direction matrices. The iterative method has been developed in [27], which can be called trilinear decomposition method. It does not require two-dimensional spatial spectrum searching or additional pairing procedure, and its performance is more excellent than that of other algorithms mentioned above.

However, all the methods mentioned above assume that both the transmit and receive arrays are well calibrated, i.e., the transmit and receive array manifolds are given explicitly. Since there exists different responses between array elements in real radar systems, the gain-phase errors may exist in transmit and receive arrays [28]–[29]. In MIMO radar systems, the performance of all algorithms aforementioned will seriously degrade the performance or be even invalid with gain-phase error [30], [31]. In order to eliminate the gain-phase errors of transmit and receive arrays in MIMO radar systems, many efforts have been devoted. An ESPRIT-like scheme has been developed in [32] for obtaining the joint angle and gain-phase error estimation, which employs the instrumental sensors method (ISM). The ESPRIT-like method is free from the operation of two-dimensional spatial spectrum searching, but the additional pairing procedure for different targets is required. On the other hand, a method based on trilinear decomposition has been presented in [33], which is called Li's method. However, its drawback is that the gain-phase error estimation has the influence of error accumulation, and the estimation performance of gain-phase error will degrade clearly, particularly in the case of low signal-to-noise ratio (SNR). Subsequently, the ESPRIT-based method is developed in [34]. The angle estimation is first achieved, and then the gain-phase errors are obtained. The performance of ESPRIT-based method is superior than that of ESPRIT-like method, and the computational complexity of ESPRIT-based method is lower than that of ESPRIT-like method. However, the performance of ESPRIT-based method can be improved further.

In this paper, we propose a tensor-based angle and gain-phase error estimation scheme in bistatic MIMO radar. Firstly, the received signal is constructed into a third-order tensor by taking advantage of the multidimensional structure of signal. Then the transmit and receive direction matrices are achieved by using the PARAFAC decomposition of third-order tensor. The gain error is estimated by taking advantage of the relationship between any two steering vectors of different angles, where the impact of phase error can be eliminated. Afterwards, the proposed method utilizes the steering vector obtained by well-calibrated sensors to estimate the DOD and DOA. Finally, the phase error estimation is achieved by utilizing the phase of all array elements, where the impact of gain error has been removed. In our algorithm, the gain and phase errors are estimated separately, in which the influence between them is eliminated. In other words, the proposed method eliminates the effect of error accumulation when estimating the parameter of gain-phase error. Therefore, the proposed algorithm achieves superior estimation accuracy compared with other methods.

The summary of this paper is shown as follows. Section II introduces the theoretical knowledge of tensor and formulates the tensor-based data model. The angle and gain-phase error estimation scheme is investigated in Section III. Simulation results are carried out in Section IV, while the conclusion is given in Section V.

Notation:$(\cdot)^*$, $(\cdot)^T$, $(\cdot)^H$, $(\cdot)^{-1}$ and $(\cdot)^\dagger$ represent conjugate, transpose, conjugate-transpose, inverse and pseudo-inverse, respectively. $\otimes$, $\odot$ and $\circ$ indicate the Kronecker product , Khatri-Rao product and outer product, respectively. $diag(\cdot)$ represents the diagonalization operation. $\Delta_n(\mathbf{A})$ denotes a diagonal matrix composed by the nth row of A. $\|\cdot\|_F$ represents the Frobenius norm. $angle(\cdot)$ stands for the phase angles for each element of the array. $min(\cdot)$ indicates the minimum element of the array. $Re(\cdot)$ is the real part for each element of the array. I_K denotes a $K \times K$ identity matrix. The n-order tensor $\mathcal{A} \in \mathbb{C}^{I_1 \times I_2 \times \ldots \times I_n}$ is denoted by symbol $[\![\cdot]\!]$ as $\mathcal{A} = [\![a_{i_1 i_2 \ldots i_n}]\!]_{i_1,\cdots,i_n=1}^{I_1,\cdots,I_n}$, where $a_{i_1 i_2 \ldots i_n}$ is the $(i_1, \cdots, i_n)$th element of the tensor.

II. THEORETICAL BASIS OF TENSOR AND TENSOR-BASED DATA MODEL

A. THEORETICAL BASIS OF TENSOR

In this part, the theoretical basis and definition of tensor are presented. The detailed introduction about the concepts and operations of tensor can be found in other literatures [35], [36].

Definition 1 (Mode-n Matrix Unfolding): Let $\mathcal{X} \in \mathbb{C}^{I_1 \times I_2 \times \ldots \times I_N}$ be a tensor, and the mode-n matrix unfolding of a tensor $\mathcal{X}$ is indicated by $[\mathcal{X}]_{(n)}$. The $(i_1, i_2, \ldots, i_N)$th element of $\mathcal{X}$ maps to the (i_n, j)th element of $[\mathcal{X}]_{(n)}$, where $j = 1 + \Sigma_{k=1,k\neq n}^{N}(i_k - 1)J_k$ with $J_k = \Pi_{m=1,m\neq n}^{k-1} I_m$.

Definition 2 (Tensor Decomposition): The parallel factor (PARAFAC) decomposition of a tensor $\mathcal{X} \in \mathbb{C}^{I_1 \times I_2 \times \ldots \times I_N}$ is shown as

$$\begin{aligned}\mathcal{X} &= \sum_{r=1}^{R} \sigma_r \mathbf{u}_r^{(1)} \circ \mathbf{u}_r^{(2)} \circ \cdots \circ \mathbf{u}_r^{(N)} \\ &= \left[\!\!\left[\boldsymbol{\sigma}; \mathbf{U}^{(1)}, \mathbf{U}^{(2)}, \ldots, \mathbf{U}^{(N)}\right]\!\!\right] \end{aligned} \tag{1}$$

where $\boldsymbol{\sigma} = [\sigma_1, \sigma_2, \ldots, \sigma_R]^{\mathrm{T}}$ is a scaling multiplier matrix, $\mathbf{U}^{(n)} = \left[\mathbf{u}_1^{(n)}, \mathbf{u}_2^{(n)}, \ldots, \mathbf{u}_R^{(n)}\right] \in \mathbb{C}^{I_n \times R}$ is a factor matrix with $\|\mathbf{u}_r^{(n)}\|_2 = 1, \forall r, n$. If the factor vector is not restricted to a unit length vector, Eq.(1) is redefined as

$$\begin{aligned}\mathcal{X} &= \sum_{r=1}^{R} \mathbf{u}_r^{(1)} \circ \mathbf{u}_r^{(2)} \circ \cdots \circ \mathbf{u}_r^{(N)} \\ &= \left[\!\!\left[\mathbf{U}^{(1)}, \mathbf{U}^{(2)}, \ldots, \mathbf{U}^{(N)}\right]\!\!\right] \end{aligned} \tag{2}$$

In particular, the PARAFAC decomposition of a third-order tensor can be called as trilinear decomposition, which is shown in Fig. 1.

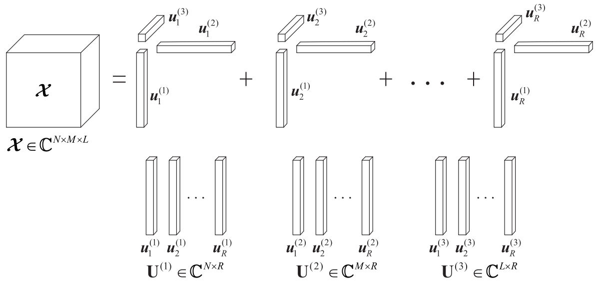

FIGURE 1. Trilinear decomposition.

B. TENSOR-BASED DATA MODEL

Consider a narrowband bistatic MIMO radar system, which equips with M-element transmit antennas and N receive antennas, and both of them are made up of half-wavelength spaced uniform linear arrays (ULA). Suppose that there are K independent targets in the far field. The direction of departure (DOD) and the direction of arrival (DOA) of the kth target can be defined as ϕ_k and θ_k, respectively. In the transmit side, all the antennas emit the orthogonal waveforms, and they can be used to form a group of matched filters. After using these matched filters to the received data, the output of matched filters can be given by [27]

$$\mathbf{x}_0(t) = [\mathbf{a}_r(\phi_1) \otimes \mathbf{a}_t(\theta_1), \ldots, \mathbf{a}_r(\phi_K) \otimes \mathbf{a}_t(\theta_K)]\mathbf{s}(t) + \mathbf{n}(t) \tag{3}$$

where $\mathbf{a}_r(\phi_k) = [1, e^{-j2\pi d_2^N \sin\phi_k}, \ldots, e^{-j2\pi d_N^N \sin\phi_k}]^{\mathrm{T}}$ is the receive steering vector, and d_n^N represents the distance between the nth receive antenna and the reference element. $\mathbf{a}_t(\theta_k) = [1, e^{-j2\pi d_2^M \sin\theta_k}, \ldots, e^{-j2\pi d_M^M \sin\theta_k}]^{\mathrm{T}}$ is the transmit steering vector, and d_m^M represents the distance between the mth transmit antenna and the reference element. $\mathbf{s}(t) = [s_1(t), s_2(t), \ldots, s_K(t)]^{\mathrm{T}} \in \mathbb{C}^{K\times 1}$ denotes the received signal vector, which is composed of phases and amplitudes of the K targets. $s_k(t) = \alpha_k(t)e^{j2\pi f_k t}$, where $\alpha_k(t)$ and f_k indicate the radar cross section (RCS) amplitude and Doppler phase shift, respectively. The noise vector is denoted as $\mathbf{n}(t)$, which is the additional white Gaussian noise vector.

However, the data model expressed in (3) is under the ideal condition where both the transmitter and receiver are well calibrated. In practical applications, the transmitter and receiver are always affected by the gain-phase error. Considering the effect of gain-phase error in both transmitter and receiver, the output of matched filter is rewritten as

$$\mathbf{x}(t) = [\hat{\mathbf{a}}_r(\phi_1) \otimes \hat{\mathbf{a}}_t(\theta_1), \ldots, \hat{\mathbf{a}}_r(\phi_K) \otimes \hat{\mathbf{a}}_t(\theta_K)]\mathbf{s}(t) + \mathbf{n}(t) \tag{4}$$

where

$$\begin{aligned}\hat{\mathbf{a}}_r(\phi_k) &= \mathbf{C}_r\mathbf{a}_r(\phi_k)\\ &= [1, e^{-j2\pi d_2^N \sin\phi_k}, \ldots, e^{-j2\pi d_n^N \sin\phi_k},\\ &\quad g_{r1}e^{-j2\pi d_{n+1}^N \sin\phi_k + j\phi_{r1}}, \ldots,\\ &\quad g_{r(N-n)}e^{-j2\pi d_N^N \sin\phi_k + j\phi_{r(N-n)}}]^{\mathrm{T}}\end{aligned} \tag{5}$$

$$\begin{aligned}\hat{\mathbf{a}}_t(\theta_k) &= \mathbf{C}_t\mathbf{a}_t(\theta_k)\\ &= [1, e^{-j2\pi d_2^M \sin\theta_k}, \ldots, e^{-j2\pi d_m^M \sin\theta_k},\\ &\quad g_{t1}e^{-j2\pi d_{m+1}^M \sin\theta_k + j\theta_{t1}}, \ldots,\\ &\quad g_{t(M-m)}e^{-j2\pi d_M^M \sin\theta_k + j\theta_{t(M-m)}}]^{\mathrm{T}}\end{aligned} \tag{6}$$

To achieve the purpose of removing the impact of gain-phase error, n and m well-calibrated sensors are added to receiver and transmitter, respectively. $\mathbf{C}_r$ and $\mathbf{C}_t$ are diagonal matrices, which contain the gain-phase errors information of transmitter and receiver, respectively. $\mathbf{C}_r$ and $\mathbf{C}_t$ can be defined as

$$\mathbf{C}_r = diag[\underbrace{1, \ldots, 1}_{n}, g_{r1}e^{j\phi_{r1}}, \ldots, g_{r(N-n)}e^{j\phi_{r(N-n)}}] \tag{7}$$

$$\mathbf{C}_t = diag[\underbrace{1, \ldots, 1}_{m}, g_{t1}e^{j\theta_{t1}}, \ldots, g_{t(M-m)}e^{j\theta_{t(M-m)}}] \tag{8}$$

According to the definition of tensor model, a third-order tensor $\mathcal{X} \in \mathbb{C}^{N\times M\times L}$ can be expressed as

$$\begin{aligned}\mathcal{X}(n, m, l) &= \sum_{k=1}^{K} \hat{\mathbf{A}}_R(n, k) \circ \hat{\mathbf{A}}_T(m, k) \circ \mathbf{S}(l, k) + \mathbf{N}_{n,m,l}\\ &\quad n = 1, 2, \ldots, N \quad m = 1, 2, \ldots, M\\ &\quad l = 1, 2, \ldots, L\end{aligned} \tag{9}$$

where $\hat{\mathbf{A}}_R(n, k)$ represents the (n, k)th element of the received direction matrix $\hat{\mathbf{A}}_R$, and $\hat{\mathbf{A}}_T(m, k)$ indicates the (m, k)th element of the transmit direction matrix $\hat{\mathbf{A}}_T$. $\mathbf{S} = [\mathbf{s}_1, \mathbf{s}_2, \ldots, \mathbf{s}_L]^{\mathrm{T}} \in \mathbb{C}^{L\times K}$ is a coefficient matrix with the lth ($l = 1, 2, \ldots, L$) row vector $\mathbf{s}_l$. $\mathbf{N}_{n,m,l}$ represents the corresponding noise matrix.

According to the definitions of Mode-n matrix unfolding and tensor decomposition, a third-order tensor $\mathcal{X} \in \mathbb{C}^{N\times M\times L}$ can be decomposed into three slices in different directions, and it is obvious that $\mathbf{X} = [\mathcal{X}]_{(3)}$, $\mathbf{Y} = [\mathcal{X}]_{(2)}$ and $\mathbf{Z} = [\mathcal{X}]_{(1)}$. Then the third-dimension slice of the tensor data $\mathcal{X} \in \mathbb{C}^{N\times M\times L}$ is given by [27]

$$\begin{aligned}[\mathcal{X}]_{(3)} &= \begin{bmatrix}\mathbf{X}_1\\ \mathbf{X}_2\\ \vdots\\ \mathbf{X}_N\end{bmatrix} = \begin{bmatrix}\hat{\mathbf{A}}_T\Delta_1(\hat{\mathbf{A}}_R)\\ \hat{\mathbf{A}}_T\Delta_2(\hat{\mathbf{A}}_R)\\ \vdots\\ \hat{\mathbf{A}}_T\Delta_N(\hat{\mathbf{A}}_R)\end{bmatrix}\mathbf{S}^{\mathrm{T}} + \begin{bmatrix}\mathbf{N}_{x1}\\ \mathbf{N}_{x2}\\ \vdots\\ \mathbf{N}_{xN}\end{bmatrix}\\ &= [\hat{\mathbf{A}}_R \odot \hat{\mathbf{A}}_T]\mathbf{S}^{\mathrm{T}} + \mathbf{N}_x\end{aligned} \tag{10}$$

where $\hat{\mathbf{A}}_T = [\hat{\mathbf{a}}_t(\theta_1), \hat{\mathbf{a}}_t(\theta_2), \ldots, \hat{\mathbf{a}}_t(\theta_K)] \in \mathbb{C}^{M\times K}$ and $\hat{\mathbf{A}}_R = [\hat{\mathbf{a}}_r(\phi_1), \hat{\mathbf{a}}_r(\phi_2), \ldots, \hat{\mathbf{a}}_r(\phi_K)] \in \mathbb{C}^{N\times K}$ represent transmit and receive direction matrices, respectively. $\mathbf{S} = [\mathbf{s}(1), \mathbf{s}(2), \ldots, \mathbf{s}(L)]^{\mathrm{T}} \in \mathbb{C}^{L\times K}$ indicates the signal matrix, $\mathbf{N}_x = [\mathbf{n}(1), \mathbf{n}(2), \ldots, \mathbf{n}(L)] \in \mathbb{C}^{MN\times L}$ is the noise matrix.

In addition, $\mathbf{X}_n$ is expressed as

$$\mathbf{X}_n = \hat{\mathbf{A}}_T\Delta_n(\hat{\mathbf{A}}_R)\mathbf{S}^{\mathrm{T}} + \mathbf{N}_{xn}, \quad n = 1, 2, \ldots, N. \tag{11}$$

Depending on the definitions of Mode-n matrix unfolding and tensor decomposition, there are two other slices of the tensor data $\mathcal{X} \in \mathbb{C}^{N\times M\times L}$, which can be denoted as [27]

$$[\mathcal{X}]_{(2)} = \begin{bmatrix} \mathbf{Y}_1 \\ \mathbf{Y}_2 \\ \vdots \\ \mathbf{Y}_M \end{bmatrix} = \begin{bmatrix} \mathbf{S}\Delta_1(\hat{\mathbf{A}}_T) \\ \mathbf{S}\Delta_2(\hat{\mathbf{A}}_T) \\ \vdots \\ \mathbf{S}\Delta_M(\hat{\mathbf{A}}_T) \end{bmatrix} \hat{\mathbf{A}}_R^{\mathrm{T}} + \begin{bmatrix} \mathbf{N}_{y1} \\ \mathbf{N}_{y2} \\ \vdots \\ \mathbf{N}_{yM} \end{bmatrix} = [\hat{\mathbf{A}}_T \odot \mathbf{S}]\hat{\mathbf{A}}_R^{\mathrm{T}} + \mathbf{N}_y \tag{12}$$

$$[\mathcal{X}]_{(1)} = \begin{bmatrix} \mathbf{Z}_1 \\ \mathbf{Z}_2 \\ \vdots \\ \mathbf{Z}_L \end{bmatrix} = \begin{bmatrix} \hat{\mathbf{A}}_R\Delta_1(\mathbf{S}) \\ \hat{\mathbf{A}}_R\Delta_2(\mathbf{S}) \\ \vdots \\ \hat{\mathbf{A}}_R\Delta_L(\mathbf{S}) \end{bmatrix} \hat{\mathbf{A}}_T^{\mathrm{T}} + \begin{bmatrix} \mathbf{N}_{z1} \\ \mathbf{N}_{z2} \\ \vdots \\ \mathbf{N}_{zL} \end{bmatrix} = [\mathbf{S} \odot \hat{\mathbf{A}}_R]\hat{\mathbf{A}}_T^{\mathrm{T}} + \mathbf{N}_z \tag{13}$$

where $\mathbf{N}_y$ and $\mathbf{N}_z$ denote the corresponding noise matrices.

III. THE PROPOSED ALGORITHM

A. DIRECTION MATRIX ESTIMATION

In this section, the direction matrix is estimated by trilinear alternating LS (TALS) method firstly, which can be utilized to achieve angle and gain-phase error estimation in the next section.

According to [37], the trilinear decomposition is utilized to estimate the direction matrices. The least squares (LS) fitting of (10) can be defined as

$$\min_{\hat{\mathbf{A}}_R,\hat{\mathbf{A}}_T,\mathbf{S}} \|\mathbf{X} - [\hat{\mathbf{A}}_R \odot \hat{\mathbf{A}}_T]\mathbf{S}^{\mathrm{T}}\|_F. \tag{14}$$

The update of matrix $\mathbf{S}$ based on LS can be expressed as

$$\tilde{\mathbf{S}}^{\mathrm{T}} = [\tilde{\hat{\mathbf{A}}}_R \odot \tilde{\hat{\mathbf{A}}}_T]^{\dagger}\mathbf{X} \tag{15}$$

where $\tilde{\hat{\mathbf{A}}}_R$ and $\tilde{\hat{\mathbf{A}}}_T$ represent the estimations of $\hat{\mathbf{A}}_R$ and $\hat{\mathbf{A}}_T$, respectively.

The LS fitting of (12) is defined as

$$\min_{\hat{\mathbf{A}}_R,\hat{\mathbf{A}}_T,\mathbf{S}} \|\mathbf{Y} - [\hat{\mathbf{A}}_T \odot \mathbf{S}]\hat{\mathbf{A}}_R^{\mathrm{T}}\|_F. \tag{16}$$

The update of matrix $\hat{\mathbf{A}}_R$ based on LS can be expressed as

$$\tilde{\hat{\mathbf{A}}}_R^{\mathrm{T}} = [\tilde{\hat{\mathbf{A}}}_T \odot \tilde{\mathbf{S}}]^{\dagger}\mathbf{Y} \tag{17}$$

where $\tilde{\hat{\mathbf{A}}}_T$ and $\tilde{\mathbf{S}}$ represent the estimations of $\hat{\mathbf{A}}_T$ and $\mathbf{S}$, respectively.

The LS fitting of Eq. (13) is defined as

$$\min_{\hat{\mathbf{A}}_R,\hat{\mathbf{A}}_T,\mathbf{S}} \|\mathbf{Z} - [\mathbf{S} \odot \hat{\mathbf{A}}_R]\hat{\mathbf{A}}_T^{\mathrm{T}}\|_F. \tag{18}$$

The update of matrix $\hat{\mathbf{A}}_T$ based on LS can be expressed as

$$\tilde{\hat{\mathbf{A}}}_T^{\mathrm{T}} = [\tilde{\mathbf{S}} \odot \tilde{\hat{\mathbf{A}}}_R]^{\dagger}\mathbf{Z} \tag{19}$$

where $\tilde{\mathbf{S}}$ and $\tilde{\hat{\mathbf{A}}}_R$ represent the estimations of $\mathbf{S}$ and $\hat{\mathbf{A}}_R$, respectively. According to Eq.(15), Eq.(17) and Eq.(19), it is clearly seen that all the matrices $\mathbf{S}$, $\hat{\mathbf{A}}_R$ and $\hat{\mathbf{A}}_T$ are updated based on LS, respectively. The iteration does not stop until the LS updates converge, and the stopping criterion is denoted as $\|\mathbf{X} - [\tilde{\hat{\mathbf{A}}}_R \odot \tilde{\hat{\mathbf{A}}}_T]\tilde{\mathbf{S}}^{\mathrm{T}}\|_F^2 \le 10^{-10}$.

For the received noisy signals, the estimated matrices ($\tilde{\hat{\mathbf{A}}}_R$, $\tilde{\hat{\mathbf{A}}}_T$, $\tilde{\mathbf{S}}$) are achieved by employing the trilinear decomposition: $\tilde{\hat{\mathbf{A}}}_R = \hat{\mathbf{A}}_R\mathbf{\Lambda}\mathbf{H}_1 + \mathbf{N}_1$, $\tilde{\hat{\mathbf{A}}}_T = \hat{\mathbf{A}}_T\mathbf{\Lambda}\mathbf{H}_2 + \mathbf{N}_2$ and $\tilde{\mathbf{S}} = \mathbf{S}\mathbf{\Lambda}\mathbf{H}_3 + \mathbf{N}_3$, where $\mathbf{\Lambda}$ represents a permutation matrix. $\mathbf{N}_1$, $\mathbf{N}_2$ and $\mathbf{N}_3$ stand for the corresponding estimation errors. $\mathbf{H}_1$, $\mathbf{H}_2$ and $\mathbf{H}_3$ are the diagonal scaling matrices, which satisfies that $\mathbf{H}_1\mathbf{H}_2\mathbf{H}_3 = \mathbf{I}_K$. In other words, after using the third-order PARAFAC decomposition process, there will exist scale ambiguity and permutation ambiguity in the results. The effect of the scale ambiguity can be removed by the operations of normalization.

B. THE GAIN ERROR ESTIMATION

In this part, the gain error is estimated by utilizing the obtained direction matrices and the special structure in the steering vectors.

Since the steering vectors of different targets have identical gain-phase error, we make the following definition by taking advantage of the relationship between any two steering vectors with different angles. Firstly, the point division operation of the steering vectors with any two angles is shown as

$$\begin{aligned}\mathbf{G}_1 &= \hat{\mathbf{a}}_r(\phi_i)./\hat{\mathbf{a}}_r(\phi_j) \\ &= [1, e^{-j2\pi d_2^N(\sin\phi_i - \sin\phi_j)}, \ldots, e^{-j2\pi d_n^N(\sin\phi_i - \sin\phi_j)}, \\ &\quad \frac{g_{ri1}}{g_{rj1}} e^{-j[2\pi d_{n+1}^N(\sin\phi_i - \sin\phi_j) - \phi_{ri1} + \phi_{rj1}]}, \ldots, \\ &\quad \frac{g_{ri(N-n)}}{g_{rj(N-n)}} e^{-j[2\pi d_N^N(\sin\phi_i - \sin\phi_j) - \phi_{ri(N-n)} + \phi_{rj(N-n)}]}]^{\mathrm{T}}\end{aligned} \tag{20}$$

where $\mathbf{G}_1$ is the result of point division operation of the steering vectors with any two angles. $\hat{\mathbf{a}}_r(\phi_i)$ is the steering vector of the ith target, $\hat{\mathbf{a}}_r(\phi_j)$ is the steering vector of the jth target. Due to the existence of scale ambiguity, the normalized operation of $\hat{\mathbf{a}}_r(\phi_i)$ and $\hat{\mathbf{a}}_r(\phi_j)$ is carried out to eliminate the influence of scale ambiguity as follows.

$$\begin{aligned}\mathbf{G}_2 &= \hat{\mathbf{a}}_r(\phi_i). * \hat{\mathbf{a}}_r^*(\phi_j) \\ &= [1, e^{-j2\pi d_2^N(\sin\phi_i - \sin\phi_j)}, \ldots, e^{-j2\pi d_n^N(\sin\phi_i - \sin\phi_j)}, \\ &\quad g_{ri1}g_{rj1}e^{-j[2\pi d_{n+1}^N(\sin\phi_i - \sin\phi_j) - \phi_{ri1} + \phi_{rj1}]}, \ldots, g_{ri(N-n)} \\ &\quad g_{rj(N-n)}e^{-j[2\pi d_N^N(\sin\phi_i - \sin\phi_j) - \phi_{ri(N-n)} + \phi_{rj(N-n)}]}]^{\mathrm{T}}\end{aligned} \tag{21}$$

where $\mathbf{G}_2$ is the result of point multiplication operation for the steering vectors of any two angles.

It can be seen from the above definition that the result of point division for any two steering vectors of different angles has the same argument with the point multiplication of the two steering vectors, but the value of modules are different. Utilizing this special relationship, we can estimate the gain error parameter while eliminate the effect of phase error, which is shown as

$$\begin{aligned}\mathbf{g}_r &= \sqrt{Re(\mathbf{G}_2)./Re(\mathbf{G}_1)} \\ &= [\underbrace{1, \ldots, 1}_{n}, g_{rj1}, \ldots, g_{rj(N-n)}]^{\mathrm{T}}.\end{aligned} \tag{22}$$

From Eq.(22), it is clearly seen that the influence of phase error is eliminated when estimating the gain error, the influence of error accumulation is eliminated, which can exhibit better estimation performance.

For the gain error $\mathbf{g}_t$ of the transmit array, the similar procedure can be applied to estimate it.

C. THE ANGLE ESTIMATION

In this part, the angle estimation is achieved without suffering from the effect of gain-phase error by utilizing the steering vectors of the well-calibrated sensors.

In order to achieve the correct angle estimation, the steering vector is obtained firstly by using the well-calibrated sensors to estimate the angle of targets. The steering vector of well-calibrated sensors is defined as

$$\bar{\mathbf{a}}_r(\phi_k) = [1, e^{-j2\pi d_2^N \sin\phi_k}, \ldots, e^{-j2\pi d_{N_r}^N \sin\phi_k}]^{\mathrm{T}}. \quad (23)$$

Then we can define that

$$\begin{aligned}\boldsymbol{\omega} &= -angle(\bar{\mathbf{a}}_r(\phi_k)) \\ &= [0, 2\pi d_2^N \sin\phi_k, \ldots, 2\pi d_{N_r}^N \sin\phi_k]^{\mathrm{T}}. \quad (24)\end{aligned}$$

The estimated steering vector of well-calibrated sensors is expressed as $\tilde{\bar{\mathbf{a}}}_r(\phi_k)$. In order to eliminate the effect of scale ambiguity, the normalization operation is applied to $\tilde{\bar{\mathbf{a}}}_r(\phi_k)$. Then $\tilde{\boldsymbol{\omega}}$ can be obtained according to Eq. (24). The estimation of $\sin\phi_k$ is achieved by using the LS principle. After that, the LS fitting is constructed as $\boldsymbol{\Pi}\mathbf{c} = \tilde{\boldsymbol{\omega}}$, where $\mathbf{c} \in \mathbb{C}^{2\times 1}$ denotes the estimated vector, $\boldsymbol{\Pi}$ is defined as

$$\boldsymbol{\Pi} = \begin{bmatrix} 1 & 0 \\ 1 & 2\pi d_2^N \\ \vdots & \vdots \\ 1 & 2\pi d_{N_r}^N \end{bmatrix} \in \mathbb{C}^{N_r\times 2}. \quad (25)$$

Then $\tilde{\mathbf{c}}$ can be achieved, which is the LS solution for $\mathbf{c}$. $\tilde{\mathbf{c}}$ is given by

$$\tilde{\mathbf{c}} = \left(\boldsymbol{\Pi}^{\mathrm{T}}\boldsymbol{\Pi}\right)^{-1}\boldsymbol{\Pi}^{\mathrm{T}}\tilde{\boldsymbol{\omega}}. \quad (26)$$

Finally, the estimation of the receive angle $\tilde{\boldsymbol{\phi}}_k$ is given by

$$\tilde{\boldsymbol{\phi}}_k = \sin^{-1}\left(\tilde{\mathbf{c}}(2)\right) \quad k = 1, 2, \ldots, K \quad (27)$$

where $\tilde{\mathbf{c}}(2)$ represents the second element of the vector $\tilde{\mathbf{c}}$.

The angle estimation of the transmit array $\tilde{\boldsymbol{\theta}}_k$ can be achieved similarly.

D. THE PHASE ERROR ESTIMATION

In this section, the estimation of phase error can be achieved by taking advantage of the relationship between the argument of $\hat{\mathbf{a}}$ and the argument of $\mathbf{a}$, where $\hat{\mathbf{a}}$ represents the steering vector affected by gain-phase error, and $\mathbf{a}$ denotes the steering vector without the influence of gain-phase error.

The argument of $\hat{\mathbf{a}}_r(\phi_k)$ can be estimated by

$$\begin{aligned}\boldsymbol{\Phi}_1 &= angle(\hat{\mathbf{a}}_r(\phi_k)) \\ &= [0, -2\pi d_2^N \sin\phi_k, \ldots, -2\pi d_n^N \sin\phi_k, -2\pi d_{n+1}^N \sin\phi_k \\ &\quad + \phi_{r1}, \ldots, -2\pi d_N^N \sin\phi_k + \phi_{r(N-n)}]^{\mathrm{T}} \quad (28)\end{aligned}$$

where $\hat{\mathbf{a}}_r(\phi_k)$ represents the received steering vector of the kth target which is affected by gain-phase error.

According to Eq.(26), the estimated vector $\tilde{\mathbf{c}}$ can be obtained. In order to obtain the argument of $\mathbf{a}_r(\phi_k)$, we define that

$$\boldsymbol{\Pi}_1 = \begin{bmatrix} 1 & 0 \\ 1 & 2\pi d_2^N \\ \vdots & \vdots \\ 1 & 2\pi d_N^N \end{bmatrix} \in \mathbb{C}^{N\times 2}. \quad (29)$$

According to the contents mentioned above, the LS fitting can be constructed as

$$\tilde{\boldsymbol{\omega}}_1 = \boldsymbol{\Pi}_1\tilde{\mathbf{c}}. \quad (30)$$

Then the argument of $\mathbf{a}$ can be denoted as

$$\begin{aligned}\boldsymbol{\Phi}_2 &= -\tilde{\boldsymbol{\omega}}_1 = angle(\mathbf{a}_r(\phi_k)) \\ &= [0, -2\pi d_2^N \sin\phi_k, \ldots, -2\pi d_n^N \sin\phi_k, -2\pi d_{n+1}^N \sin\phi_k, \\ &\quad \ldots, -2\pi d_N^N \sin\phi_k]^{\mathrm{T}} \quad (31)\end{aligned}$$

where $\mathbf{a}_r(\phi_k)$ indicates the received steering vector of the kth target which is not affected by gain-phase error.

Finally, the estimation of the received array phase error can be given by

$$\begin{aligned}\mathbf{p}_r &= \boldsymbol{\Phi}_1 - \boldsymbol{\Phi}_2 \\ &= [\underbrace{0, \ldots, 0}_{n}, \phi_{r1}, \ldots, \phi_{r(N-n)}]^{\mathrm{T}}. \quad (32)\end{aligned}$$

It can be clearly seen that the effect of gain error has been eliminated and the phase error estimation is not influenced by the gain error. Thus our approach can remove the influence of error accumulation, and the estimation of phase error is more accurate.

By using the method mentioned above, the estimation for phase error $\mathbf{p}_t$ of the transmit array is obtained.

IV. ADVANTAGES OF OUR METHOD

The advantages of our method can be summarized as follows:

(1) Our method can eliminate the influence of error accumulation and obtain better estimation performance.

(2) There is no spatial spectrum searching and eigenvalue decomposition when estimating angle and gain-phase errors, so our algorithm has low computational complexity.

(3) Our approach can achieve angles with automatic paired without additional angle pairing process.

(4) Compared with ESPRIT-like method [32], ESPRIT-based method [34]and Li's method [33], the proposed method achieves better angle and gain-phase error estimation performance, which is shown in the simulation part.

V. SIMULATION RESULTS

In this part, some numerical experiments are provided to validate the effectiveness and superiority of our approach. The ESPRIT-like method [32], Li's method [33], ESPRIT-based method [34] and Cramer-Rao bound (CRB) [38] are compared with our algorithm. In this paper, the bistatic MIMO radar with $M = 8$ transmit antennas and $N = 6$ received antennas is considered. In this part, except for especially pointing out, it is assumed that there are $K = 3$ uncorrelated targets. The three targets are situated at $(\phi_1, \theta_1) = (-5°, 10°)$, $(\phi_2, \theta_2) = (15°, 20°)$, $(\phi_3, \theta_3) = (35°, 0°)$. In all numerical experiments, by taking into account the impact of gain-phase error in transmitter and receiver, the gain-phase error coefficients are given stochastically by: $\mathbf{c}_t = [1, 1, 1, 1.21e^{j0.12}, 1.1e^{j1.35}, 0.89e^{j0.98}, 1.35e^{j2.65}, 0.92e^{j1.97}]$ and $\mathbf{c}_r = [1, 1, 0.94e^{j1.12}, 1.23e^{j2.35}, 1.49e^{j0.58}, 0.75e^{j0.65}]$. The root mean square error (RMSE) is employed to assess the performance of the proposed method, and the RMSE of the angle estimation can be denoted as

$$\mathrm{RMSE} = \frac{1}{K}\sum_{k=1}^{K}\sqrt{\frac{1}{\zeta}\sum_{i=1}^{\zeta}\left\{\left(\tilde{\theta}_{k,i} - \theta_k\right)^2 + \left(\tilde{\phi}_{k,i} - \phi_k\right)^2\right\}} \tag{33}$$

where $\tilde{\theta}_{k,i}$ and $\tilde{\phi}_{k,i}$ represent the estimation of θ_k and ϕ_k for the ith Monte Carlo test, respectively. ζ denote the total amount of Monte Carlo tests, and $\zeta = 500$ is used in these simulations.

In addition, the RMSE of the array gain-phase error estimation is defined as

$$\mathrm{RMSE} = \sqrt{\frac{1}{\zeta}\sum_{i=1}^{\zeta}\left\{\left\|\tilde{\mathbf{c}}_{t,i} - \mathbf{c}_t\right\|_F^2 + \left\|\tilde{\mathbf{c}}_{r,i} - \mathbf{c}_r\right\|_F^2\right\}} \tag{34}$$

where $\tilde{\mathbf{c}}_{t,i}$ and $\tilde{\mathbf{c}}_{r,i}$ indicate the estimation of $\mathbf{c}_t$ and $\mathbf{c}_r$ for the ith Monte Carlo test, respectively.

Another metric employed to assess the performance of our method is the probability of the successful detection (PSD), which can be defined as

$$\mathrm{PSD} = \frac{D}{\zeta} \times 100\% \tag{35}$$

where D indicates the total amount of successful tests, and the definition of a successful experiment is that the absolute error of all numerical experiments are less than $\min[(\tilde{\theta}_k - \theta_k)_{k=1}^{K}, (\tilde{\phi}_k - \phi_k)_{k=1}^{K}]$.

Fig. 2 and Fig. 3 show the estimation results of the proposed method with SNR=20dB, and the number of snapshots is L=100. In Fig. 2 and Fig. 3, we can clearly see that the estimations of angles and gain-phase error are obtained correctly, which verifies the effectiveness of our algorithm.

The first experiment investigates the relationship between RMSE and SNR of angle estimation (shown in Fig. 4) and gain-phase error estimation (shown in Fig. 5). The number of snapshots is L=100. In this simulation, we compare the performance of our method with Li's method, the ESPRIT-based method, the ESPRIT-like method and CRB. In Fig. 4 and Fig. 5, it can be clearly known that the estimation performance of our algorithm is better to Li's method, the ESPRIT-based method and the ESPRIT-like method, and the performance of our method is closer

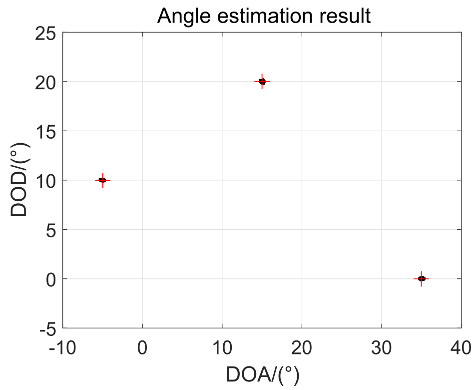

FIGURE 2. Angle estimation performance of the proposed algorithm with SNR=20dB.

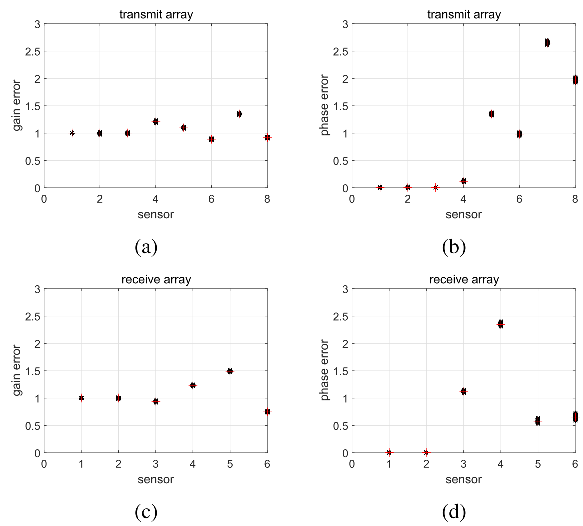

FIGURE 3. Gain-phase error estimation performance of the proposed algorithm with SNR=20dB.

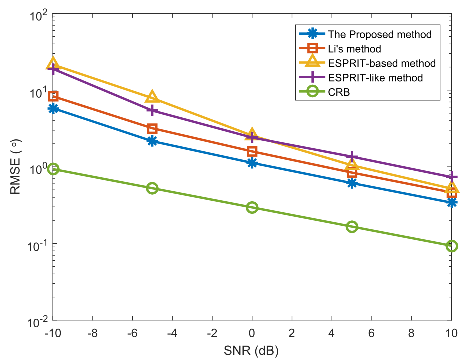

FIGURE 4. The contrast of angle estimation RMSE versus SNR.

to CRB. The estimation obtained by Li's method using trilinear decomposition has the effect of error accumulation, and thus the performance is limited. The proposed method utilizes multi-dimensional characteristics of the signal to eliminate the error accumulation effect, so the performance of the proposed algorithm is better than that of other algorithms. For the ESPRIT-based method, the performance of angle

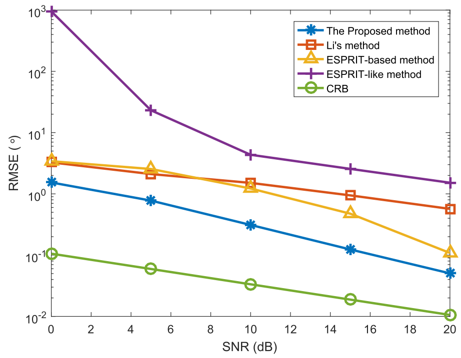

FIGURE 5. The contrast of gain-phase error estimation RMSE versus SNR.

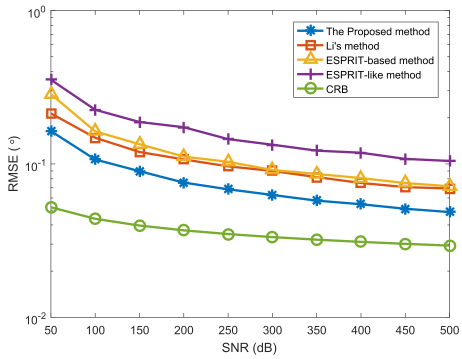

FIGURE 6. The contrast of angle estimation RMSE versus the number of snapshots.

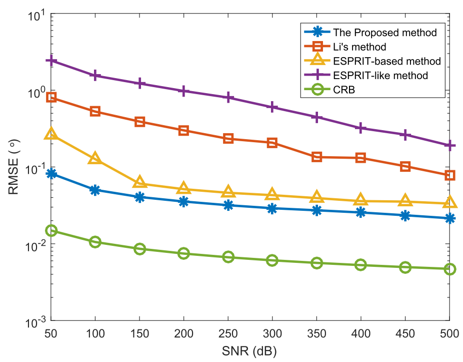

FIGURE 7. The contrast of gain-phase error estimation RMSE versus the number of snapshots.

estimation is worse than that of Li's method at high SNR, but its performance of gain-phase error estimation is better than that of Li's method. Furthermore, the performance of Li's algorithm is more outstanding than that of the ESPRIT-like algorithm, and the main reason is that Li's method estimates the gain-phase errors by transforming the estimation into an issue of convex optimization.

The second experiment displays the relationship between RMSE and the number of snapshots with SNR=20dB. The performance of different algorithms is demonstrated in two aspects: angle estimation (shown in Fig. 6) and gain-phase error estimation (shown in Fig. 7). Li's algorithm, the ESPRIT-based algorithm, the ESPRIT-like algorithm and CRB are compared with our method. It can be known from

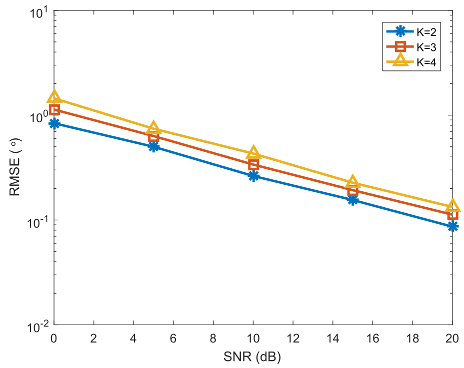

FIGURE 8. The contrast of angle estimation RMSE versus SNR with different value of K.

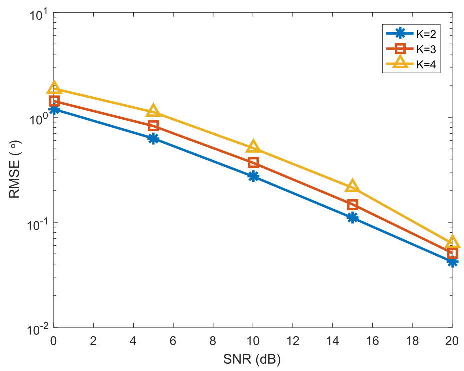

FIGURE 9. The contrast of gain-phase error estimation RMSE versus SNR with different value of K.

Fig. 6 and Fig. 7 that the performance of all methods is gradually promoting with the augment of the number of snapshots, where the performance of our method is more outstanding than that of other methods. This is because our method makes use of the multi-dimensional structure of the signal and eliminates the effect of error accumulation. For the ESPRIT-based method, the performance of angle estimation is worse than that of Li's method, but its performance of gain-phase error estimation is superior than that of Li's method. Moreover, the ESPRIT-like algorithm has the worst performance.

In the third experiment, we investigate the angle estimation performance (shown in Fig. 8) and the gain-phase errors estimation performance (shown in Fig. 9) with different number of targets. The number of snapshots is L=100. It is shown from Fig. 8 and Fig. 9 that the estimation performance of our method degrades with the increasing number of targets.

In the fourth experiment, the impacts of the number of transmitter and receiver for the performance of angle estimation are evaluated. The number of snapshots is L=50. The angle estimation performance under different numbers of receive antennas is depicted in Fig. 10. Fig. 11 shows the proposed method angle estimation performance with different number of transmit antennas. It can be known from Fig. 10 and Fig. 11 that the angle estimation performance of our method will be improved with the increasing number of transmitter or receiver. The reason is that more number of

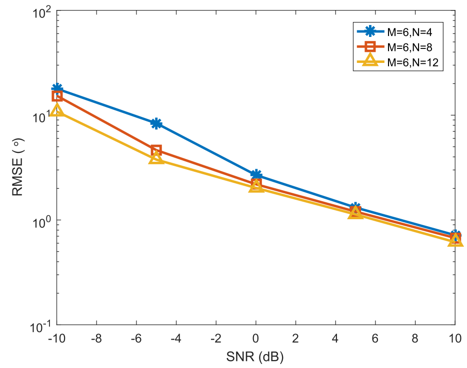

FIGURE 10. RMSE of angle estimation versus SNR with different value of N.

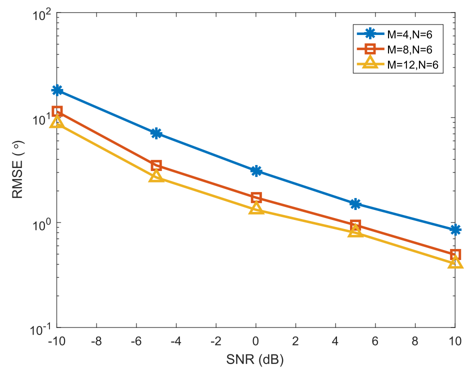

FIGURE 11. RMSE of angle estimation versus SNR with different value of M.

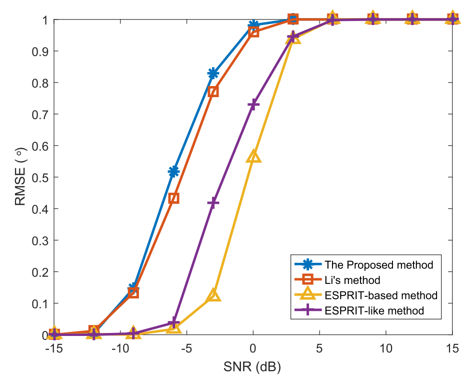

FIGURE 12. Probability of successful detection versus SNR with different algorithms.

antennas contained in transmit or receive arrays can obtain more spatial diversity gain.

The fifth experiment depicts the PSD of the angle estimation versus SNR for three targets with $L=100$. In this simulation, the performance of our method is compared with Li's method, the ESPRIT-based method and the ESPRIT-like method. From Fig. 12, it can be seen that PSD of all the algorithms will turn higher with the increasing of SNR, and eventually reach 100% in the case of high enough SNR. It is worth noting that the PSD of our algorithm can reach 100% with relatively low SNR compared with other algorithms. On the other hand, the PSD of our algorithm is close to that of Li's method at low SNR. In addition, it is clear that Li's method has superior PSD than the ESPRIT-like algorithm and the ESPRIT-based method. Although the PSD of the ESPRIT-based algorithm can reach 100%, its SNR threshold is very high.

VI. CONCLUSION

In this paper, a tensor-based angle and array gain-phase error estimation scheme is proposed in bistatic MIMO radar. The proposed method applies the (PARAFAC) decomposition technique to achieve the direction matrices, and the effect of error accumulation is eliminated in the procedure of angle and gain-phase error estimation. Thus, compared with existing methods, the proposed method exhibits superior angle and gain-phase error estimation performance. The superiority of our algorithm is validated by numerical experiments.

REFERENCES

[1] E. Fishler, A. Haimovich, R. Blum, D. Chizhik, L. Cimini, and R. Valenzuela, "MIMO radar: An idea whose time has come," *Proc. IEEE*, vol. 7, no. 6, pp. 71–78, Apr. 2004.
[2] H. Krim and M. Viberg, "Two decades of array signal processing research: The parametric approach," *IEEE Signal Process. Mag.*, vol. 13, no. 4, pp. 67–94, Jul. 1996.
[3] E. Fishler, A. Haimovich, R. Blum, L. Cimini, D. Chizhik, and R. Valenzuela, "Performance of MIMO radar systems: Advantages of angular diversity," in *Proc. 38th Asilomar Conf. Signals, Syst., Comput.*, vol. 1, Nov. 2004, pp. 305–309.
[4] J. Li and P. Stoica, "MIMO radar with colocated antennas," *IEEE Signal Process. Mag.*, vol. 24, no. 5, pp. 106–114, Sep. 2007.
[5] A. A. Gorji, R. Tharmarasa, and T. Kirubarajan, "Optimal antenna allocation in MIMO radars with collocated antennas," *IEEE Trans. Signal Process.*, vol. 500, no. 1, pp. 542–558, Jan. 2014.
[6] A. Hassanien and S. A. Vorobyov, "Phased-MIMO radar: A tradeoff between phased-array and MIMO radars," *Signal Process.*, vol. 58, no. 6, pp. 3137–3151, Jun. 2010.
[7] E. Fishler, A. Haimovich, and R. Blum, "Spatial diversity in radars-models and detection performance," *IEEE Trans. Signal Process.*, vol. 54, no. 3, pp. 823–838, Mar. 2006.
[8] A. M. Haimovich, R. S. Blum, and L. J. Cimini, "MIMO radar with widely separated antennas," *IEEE Signal Process. Mag.*, vol. 25, no. 1, pp. 116–129, Jan. 2008.
[9] L. Wan, X. Kong, and F. Xia, "Joint range-Doppler-angle estimation for intelligent tracking of moving aerial targets," *IEEE Internet Things J.*, vol. 5, no. 3, pp. 1625–1636, Jun. 2018.
[10] X. Wang, M. Huang, C. Shen, and D. Meng, "Robust vehicle localization exploiting two based stations cooperation: A MIMO radar perspective," *IEEE Access*, vol. 6, pp. 48747–48755, 2018.
[11] X. P. Wang, D. D. Meng, and M. X. Huang, "Reweighted regularized sparse recovery for DOA estimation with unknown mutual coupling," *IEEE Commun. Lett.*, vol. 23, no. 2, pp. 290–293, Feb. 2019.
[12] F. Wen, Z. Zhang, and X. Zhang, "CRBs for direction-of-departure and direction-of-arrival estimation in collocated MIMO radar in the presence of unknown spatially coloured noise," *IET Radar, Sonar Navigat.*, vol. 13, no. 2, pp. 249–257, 2019.
[13] H. Yan, J. Li, and G. Liao, "Multitarget identification and localization using bistatic MIMO radar systems," *EURASIP J. Adv. Signal Process.*, vol. 2008, Jan. 2008, Art. no. 48.
[14] X. F. Zhang and D. Z. Xu, "Angle estimation in bistatic MIMO radar using improved reduced dimension Capon algorithm," *J. Syst. Eng. Electron.*, vol. 24, no. 1, pp. 84–89, Feb. 2013.
[15] X. Gao, X. Zhang, G. Feng, Z. Wang, and D. Xu, "On the MUSIC-derived approaches of angle estimation for bistatic MIMO radar," in *Proc. Int. Conf. Wireless Netw. Inf. Syst.*, Dec. 2009, pp. 343–346.
[16] A. Zahernia, M. J. Dehghani, and R. Javidan, "MUSIC algorithm for DOA estimation using MIMO arrays," in *Proc. Int. Conf. Telecommun. Syst., Services, Appl.*, Oct. 2011, pp. 149–153.
[17] X. Zhang, L. Xu, and L. Xu, "Direction of departure (DOD) and direction of arrival (DOA) estimation in MIMO radar with reduced-dimension MUSIC," *IEEE Commun. Lett.*, vol. 14, no. 12, pp. 1161–1163, Dec. 2010.

[18] D. Chen, B. Chen, and G. Qin, "Angle estimation using ESPRIT in MIMO radar," *Electron. Lett.*, vol. 44, no. 12, pp. 770–771, Jun. 2008.

[19] C. Jinli, G. Hong, and S. Weimin, "Angle estimation using ESPRIT without pairing in MIMO radar," *Electron. Lett.*, vol. 44, no. 24, pp. 1422–1423, Nov. 2008.

[20] H. Zheng, B. Chen, and M. Yang, "Unitary ESPRIT algorithm for bistatic MIMO radar," *Electron. Lett.*, vol. 48, no. 3, pp. 179–181, Feb. 2012.

[21] J. Chen, H. Gu, and W. Su, "A new method for joint DOD and DOA estimation in bistatic MIMO radar," *Signal Process.*, vol. 90, no. 2, pp. 714–718, 2010.

[22] M. Jin, G. S. Liao, and J. Li, "Joint DOD and DOA estimation for bistatic MIMO radar," *Signal Process.*, vol. 89, no. 2, pp. 244–251, Feb. 2009.

[23] D. Nion and N. D. Sidiropoulos, "A PARAFAC-based technique for detection and localization of multiple targets in a MIMO radar system," in *Proc. IEEE Int. Conf. Acoust., Speech Signal Process. (ICASSP)*, Apr. 2009, pp. 2077–2080.

[24] D. Nion and N. D. Sidiropoulos, "Adaptive algorithms to track the PARAFAC decomposition of a third-order tensor," *IEEE Trans. Signal Process.*, vol. 57, no. 6, pp. 2299–2310, Jun. 2009.

[25] D. Nion and N. D. Sidiropoulos, "Tensor algebra and multidimensional harmonic retrieval in signal processing for MIMO radar," *IEEE Trans. Signal Process.*, vol. 58, no. 11, pp. 5693–5705, Nov. 2010.

[26] B. Xu, Y. Zhao, Z. Cheng, and H. Li, "A novel unitary PARAFAC method for DOD and DOA estimation in bistatic MIMO radar," *Signal Process.*, vol. 138, pp. 273–279, 2017.

[27] X. Zhang, Z. Xu, L. Xu, and D. Xu, "Trilinear decomposition-based transmit angle and receive angle estimation for multiple-input multiple-output radar," *IET Radar, Sonar Navigat.*, vol. 5, no. 6, pp. 626–631, Jul. 2011.

[28] E. Tuncer and B. Freidlander, "Calibration in array processing," in *Classical and Modern Direction-of-Arrival Estimation*. Amsterdam, The Netherlands: Elsevier, 2009.

[29] A. Liu, G. Liao, C. Zeng, Z. Yang, and Q. Xu, "An eigenstructure method for estimating DOA and sensor gain-phase errors," *IEEE Trans. Signal Process.*, vol. 59, no. 12, pp. 5944–5956, Dec. 2011.

[30] B. Liao, J. Wen, L. Huang, C. Guo, and S.-C. Chan, "Direction finding with partly calibrated uniform linear arrays in nonuniform noise," *IEEE Sensors J.*, vol. 16, no. 12, pp. 4882–4890, Jun. 2016.

[31] J. Jiang, F. Duan, J. Chen, Z. Chao, Z. Chang, and X. Hua, "Two new estimation algorithms for sensor gain and phase errors based on different data models," *IEEE Sensors J.*, vol. 13, no. 5, pp. 1921–1930, May 2013.

[32] Y. D. Guo, Y. S. Zhang, and N. N. Tong, "ESPRIT-like angle estimation for bistatic MIMO radar with gain and phase uncertainties," *Electron. Lett.*, vol. 47, no. 17, pp. 996–997, Aug. 2011.

[33] J. F. Li, X. F. Zhang, and X. Gao, "A joint scheme for angle and array gain-phase error estimation in bistatic MIMO radar," *IEEE Geosci. Remote Sens. Lett.*, vol. 10, no. 6, pp. 1478–1482, Nov. 2013.

[34] J. Li, M. Jin, Y. Zheng, G. Liao, and L. Lv, "Transmit and receive array gain-phase error estimation in bistatic MIMO radar," *IEEE Antennas Wireless Propag. Lett.*, vol. 14, pp. 32–35, 2015.

[35] L. De Lathauwer, B. De Moor, and J. Vandewalle, "A multilinear singular value decomposition," *SIAM J. Matrix Anal. Appl.*, vol. 21, no. 4, pp. 1253–1278, 2000.

[36] T. G. Kolda and B. W. Bader, "Tensor decompositions and applications," *SIAM Rev.*, vol. 51, no. 3, pp. 455–500, Aug. 2009.

[37] J. B. Kruskal, "Three-way arrays: Rank and uniqueness of trilinear decompositions, with application to arithmetic complexity and statistics," *Linear Algebra Appl.*, vol. 18, no. 2, pp. 95–138, 1975.

[38] P. Stoica and A. Nehorai, "Performance study of conditional and unconditional direction-of-arrival estimation," *IEEE Trans. Acoust., Speech Signal Process.*, vol. 38, no. 10, pp. 1783–1795, Oct. 1990.

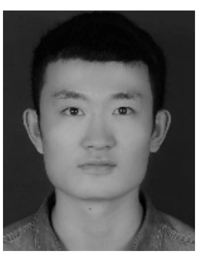

YUEHAO GUO was born in 1996. He received the B.S. degree from Hainan University, Haikou, China, in 2017, where he is currently pursuing the M.S. degree in electronics and communication engineering. His research interests include array signal processing and MIMO radar.

XIANPENG WANG was born in 1986. He received the M.S. and Ph.D. degrees from the College of Automation, Harbin Engineering University (HEU), Harbin, China, in 2012 and 2015, respectively. He was a full-time Research Fellow with the School of Electrical and Electronic Engineering, Nanyang Technological University, Singapore, from 2015 to 2016. He is currently a Professor with the College of Information Science and Technology, Hainan University. He has authored over 60 papers published in related journals and international conference proceedings, and has served as a reviewer of over 20 journals. His major research interests include communication systems, array signal processing, radar signal processing, and compressed sensing and its applications.

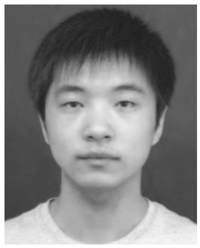

LIANGTIAN WAN (M'15) received the B.S. and Ph.D. degrees from the College of Information and Communication Engineering, Harbin Engineering University, Harbin, China, in 2011 and 2015, respectively. From 2015 to 2017, he was a Research Fellow with the School of Electrical and Electrical Engineering, Nanyang Technological University, Singapore. He is currently an Associate Professor with the School of Software, Dalian University of Technology, China. He has published over 40 scientific papers in international journals and conferences. He is an Associate Editor of the IEEE ACCESS. His research interests include social network analysis and mining, big data, array signal processing, wireless sensor networks, and compressive sensing and its application.

MENGXING HUANG received the Ph.D. degree from Northwestern Polytechnical University, in 2007. He then joined as a Postdoctoral Researcher with the Research Institute of Information Technology, Tsinghua University. In 2009, he joined Hainan University, where he is currently a Professor and a Ph.D. Supervisor of computer science and technology, and the Dean of the College of Information Science and Technology. He is also the Executive Vice-President of the Hainan Province Institute of Smart City, and the Leader of the Service Science and Technology Team, Hainan University. He has published more than 60 academic papers as the first or corresponding author. He has reported 12 patents of invention, owns three software copyright, and published two monographs and two translations. His current research interests include signal processing for sensor systems, big data, and intelligent information processing. He received 1 Second Class and 1 Third Class Prizes of The Hainan Provincial Scientific and Technological Progress.

CHONG SHEN was born in 1981. He received the Ph.D. degree from the Cork Institute of Technology, Ireland, in 2008. He was a full-time Postdoctoral Research Fellow with the Tyndall National Institute, Ireland, from 2008 to 2009. He is currently a Professor with the College of Information Science Technology, Hainan University. He has authored over 100 papers published in related journals and international conference proceedings, and has served as a reviewer for over 10 journals. His major research interests include array signal processing, ultra-wideband communications, wireless communications, sensor networks and the Internet of things, and embedded systems research.

KUN ZHANG was born in 1981. He is currently pursuing the Ph.D. degree with the College of Information Science and Technology, Hainan University, Haikou, China. He is currently a Professor with the College of Ocean Information Engineering, Hainan Tropical Ocean University. He has authored over 100 papers published in related journals. His major research interests include intelligent data analysis and data mining, ultra-wideband communications, wireless communications, sensor networks and the Internet of Things, and embedded systems.

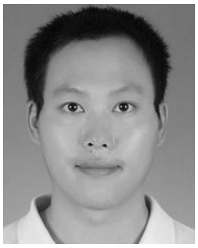

YONGQIN YANG was born in 1984. He received the Ph.D. degree from the School of Physics, Sun Yat-sen University, Guangdong, China. He is currently a Lecturer with the College of Information Science and Technology, Hainan University, Haikou, China. He has authored over 100 papers published in related journals. His major research interests include signal processing and wireless communications, and sensor networks.